

## Pairing in cuprates from high-energy electronic states

A. F. SANTANDER-SYRO<sup>1</sup>, R. P. S. M. LOBO<sup>1</sup>, N. BONTEMPS<sup>1(\*)</sup>,  
Z. KONSTANTINOVIC<sup>2</sup>, Z. Z. LI<sup>2</sup> and H. RAFFY<sup>2</sup>

<sup>1</sup> *Laboratoire de Physique du Solide, CNRS UPR 5  
Ecole Supérieure de Physique et Chimie Industrielles de la Ville de Paris  
75231 Paris cedex 5, France*

<sup>2</sup> *Laboratoire de Physique des Solides, CNRS UMR 8502, Université Paris-Sud  
91405 Orsay cedex, France*

(received 22 July 2002; accepted in final form 19 March 2003)

PACS. 74.25.-q – Properties of type I and type II superconductors.

PACS. 74.25.Gz – Optical properties.

PACS. 74.72.Hs – Bi-based cuprates.

**Abstract.** – The *in-plane* optical conductivity of  $\text{Bi}_2\text{Sr}_2\text{CaCu}_2\text{O}_{8+\delta}$  films with small carrier density (underdoped) up to large carrier density (overdoped) is derived from accurate reflectivity data. Integrating the conductivity up to increasingly higher frequencies yields the energy scale involved in the formation of the condensate. At least in the underdoped sample, states extending up to 2 eV contribute to the superfluid. This anomalously large energy scale may be assigned to a change of *in-plane* kinetic energy at the superconducting transition, and is compatible with an electronic pairing mechanism.

In conventional superconductors, electrons bind into Cooper pairs by exchanging a phonon. The condensation of pairs leads to the zero-resistance superconducting state. In cuprate superconductors, however, the binding mechanism remains an open question. One key issue is the typical energy scale of the excitations responsible for pairing. Infrared (IR) and visible spectroscopy measures the charge density distribution as a function of energy, through the investigation of the area under the frequency ( $\omega$ ) and temperature ( $T$ ) dependent optical conductivity  $\sigma_1(\omega, T)$ . This area, known as the spectral weight  $W$ , is defined as

$$W = \int_{0^+}^{\omega_c} \sigma_1(\omega, T) d\omega, \quad (1)$$

where  $\omega_c$  is a cut-off frequency. When integrating from zero to infinite frequency, this spectral weight should be conserved as it depends only on the total charge density and the bare electronic mass. Ferrell, Glover and Tinkham (FGT) noted that, in the superconducting state, the spectral weight  $\Delta W$  lost from the finite frequency conductivity is retrieved in the spectral weight  $W_s$  of the  $\delta(\omega)$  function centered at zero frequency, representing the condensate [1]. Actually,  $\Delta W$  is approximately equal to  $W_s$  (the so-called FGT sum rule) as soon as the cut-off

---

(\*) E-mail: [Nicole.Bontemps@espci.fr](mailto:Nicole.Bontemps@espci.fr)

frequency  $\omega_c$  in eq. (1) covers the spectrum of excitations responsible for the pairing mechanism. In conventional superconductors, this occurs at an energy corresponding roughly to  $4\Delta$  ( $\Delta$  is the superconducting gap, related in BCS theory to the Debye frequency) [1]. Assuming a similar behaviour in cuprates, the FGT rule should be exhausted at  $\hbar\omega_c \sim 0.1$  eV, as a typical maximum gap value in these *d*-wave superconductors is roughly 25 meV [2]. A violation of this sum rule, *i.e.*  $\Delta W < W_s$  when integrating up to 0.1 eV, was reported for the interlayer optical conductivity of some cuprate superconductors [3–5], and discussed as possibly related to a change of interlayer kinetic energy. This question has indeed raised active experimental and theoretical discussions [6–9], connected in particular with the interlayer tunneling theory [10].

To date there is no experiment showing such unconventional behaviour directly for the in-plane conductivity of cuprates. Nevertheless, this point was also given a renewed interest [11–13]. What is at stake is that the need of an energy scale higher than any typical phonon energy to exhaust the FGT rule would be the hallmark of an electronic mediated pairing mechanism. Most of the changes observed below the critical temperature  $T_c$  in the in-plane optical response at large energy scales are inconclusive [14–16]. Only very recently, visible ellipsometry showed that in-plane spectral weight is lost at visible wavelengths at the superconducting transition [17].

This paper demonstrates, from a thorough study of the FGT sum rule of the in-plane conductivity, that at least in underdoped  $\text{Bi}_2\text{Sr}_2\text{CaCu}_2\text{O}_{8+\delta}$  (Bi-2212), an electronic energy scale is indeed involved when the material becomes superconducting.

Three films from the Bi-2212 family were selected at three doping levels which probe three typical locations in the phase diagram: the underdoped (UD), the optimally doped (OPD) and the overdoped (OD) regime. We find that in the UD sample, one must integrate the optical conductivity up to  $\sim 16000 \text{ cm}^{-1}$  (2 eV), in order to retrieve the condensate spectral weight. Such an energy scale is much larger than typical boson energies in a solid hence suggesting an electronic pairing mechanism. In the OD and OPD samples, our error bars do not allow us to extract an unconventional energy scale.

The three films were epitaxially grown by r.f. magnetron sputtering on (100)  $\text{SrTiO}_3$  substrates. The maximum critical temperature (defined at zero resistance) obtained in these conditions is  $\sim 84$  K. The OD and UD states were obtained by post-annealing the films in a controlled atmosphere [18]. X-ray analyses confirmed that the films are single phase. Our films critical temperatures are 70 K (UD), 80 K (OPD) and 63 K (OD). The film thicknesses, determined by Rutherford Back Scattering (RBS) for the OPD and OD samples are 395 nm and 270 nm [19]. A lower bound for the UD sample was estimated by RBS in a sample grown on MgO simultaneously to ours, yielding 220 nm. The optical homogeneity for the three films was verified by infrared microscopy with a lateral resolution of  $20 \mu\text{m}$ . The reflectivities, taken at 15 temperatures between 300 K and 10 K, were measured in the spectral range  $[30\text{--}7000] \text{ cm}^{-1}$  with a Fourier transform spectrometer, supplemented with standard visible spectroscopy in the range  $[4000\text{--}25000] \text{ cm}^{-1}$ . Using films rather than single crystals allows to measure relative variations in reflectivity within less than 0.2%, even in the visible range, due to their large surface (typically  $6 \times 6 \text{ mm}^2$ ).

It is known that temperature changes of the optical response in the mid-infrared and the visible ranges are small, but cannot be neglected [20]. Yet, as pointed out in ref. [16], most studies rely on a single spectrum at one temperature in the visible range. We did monitor the temperature evolution of the reflectivity spectra in the full available range. This is obviously important if one is looking for a spectral-weight transfer originating from (or going to) any part of the *whole* frequency range.

The contribution of the substrate to the experimentally measured reflectivities precludes the Kramers-Kronig analysis in thin films. In order to extract the optical functions intrinsic

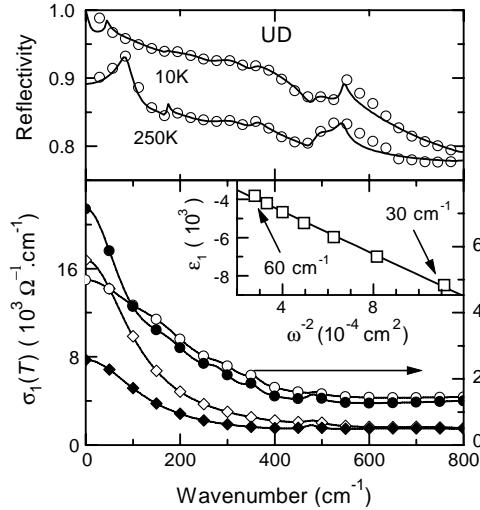


Fig. 1 – Top panel: measured reflectivity spectra of the underdoped sample at 250 K and 10 K (open symbols) and fitted spectra (solid lines). Three peaks from the SrTiO<sub>3</sub> substrate are visible at 60, 180 and 530 cm<sup>-1</sup>. The fits lie within  $\pm 0.5\%$  of the raw data in the full spectral range (up to 25000 cm<sup>-1</sup>), except at  $620 \pm 50$  cm<sup>-1</sup>, where the deviation is 1%. Bottom panel: real part of the calculated conductivity above  $T_c$  (open symbols) and at 10 K (full symbols) for the UD (right scale) and OD (left scale) samples. The conductivities are extrapolated from 30 cm<sup>-1</sup> down to zero as a result of the fit. Inset: linear fit (solid line) of the low-frequency  $\epsilon_1(\omega, T < T_c)$  data from the UD sample (open squares), *vs.*  $\omega^{-2}$ .

to Bi-2212, we simulated its dielectric function at each temperature and doping level using Drude-Lorentz oscillators (thus warranting causality). We then modelled the reflectance of the film on top of a substrate, using the optical constants of SrTiO<sub>3</sub> experimentally determined at each temperature [21]. Finally, we adjusted the attempt dielectric function in order to fit accurately the raw reflectivity spectra. Examples of such fits are shown in the top panel of fig. 1. Once the dielectric function is known, we can generate any other optical function, in particular the optical conductivity. A relative error  $\Delta R/R$  in the fit yields a relative error magnified by a factor 10 in the real part of the conductivity provided that  $\Delta R/R \ll 1$ . This relative error spreads over twice the range where the deviation to the raw data occurs. The thicknesses of the films are also determined by the fit. Fits are accurate within less than 0.5% taking 241, 434 and 297 Å for the UD, OPD and OD samples, respectively. These values differ by less than 10% from the RBS data and less than 5% from a more accurate electronic-microscopy image taken on the UD sample. We checked that the associated error in the conductivity is less than 10%. The fit yields a valuable extrapolation of the conductivity in the low-energy range ( $\omega < 30$  cm<sup>-1</sup>, not available experimentally) [22], which is important in the evaluation of the spectral weight. In this range however, the relative error in the conductivity was calculated and reaches 20% [23].

The conductivities at  $T_A \geq T_c$  and  $T_B < T_c$  are shown in fig. 1 (lower panel), up to 800 cm<sup>-1</sup> (0.1 eV) for the UD ( $T_A = 80$  K) and OD ( $T_A = 70$  K) samples, respectively. In both cases,  $T_B = 10$  K. In the OD sample, the curve  $\sigma_1(\omega, T \leq T_c)$  lies below the one at  $T \geq T_c$ , exhibiting an expected loss of spectral weight in this energy range. In contrast, the curve  $\sigma_1(\omega, T \leq T_c)$  for the UD sample lies *above* the one at  $T \geq T_c$ , up to 100 cm<sup>-1</sup>, then crosses it, and no loss of spectral weight is apparent in the energy range shown.

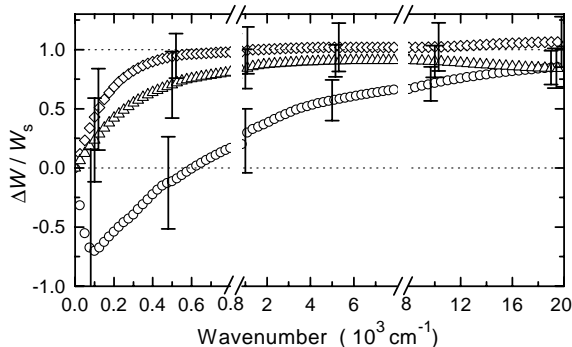


Fig. 2 – Ratio  $\Delta W/W_s$  vs. frequency showing the exhaustion of the FGT sum rule at conventional energies for the OD (diamonds, right error bars) and OPD (triangles, middle error bars) samples. An unconventional ( $\sim 16000 \text{ cm}^{-1}$  or  $2 \text{ eV}$ ) energy scale is required for the UD sample (circles, left error bars). Note that the frequency scale changes at  $800$  and  $8000 \text{ cm}^{-1}$ .

From an experimental point of view, the FGT sum rule usually compares the change  $\Delta W = W(T_A) - W(T_B)$  (eq. (1)) and the superfluid spectral weight  $W_s$ .  $W_s$  was determined for  $T < T_c$  at low frequencies, within the measured spectral range, by looking at the region where the real part of the dielectric function  $\varepsilon_1(\omega)$  behaves linearly when plotted vs.  $1/\omega^2$  (London approximation). An example is shown in the inset of fig. 1. The slope is directly related to the superfluid spectral weight  $W_s$  through the “London” frequency  $\Omega_L = c/\lambda_L$ , where  $\lambda_L$  is the London penetration depth. At  $10 \text{ K}$ , for instance, we find  $\Omega_L = 7200 \text{ cm}^{-1}$  and  $2350 \text{ cm}^{-1}$  for the OD and UD samples, respectively. The value for the OD sample is in fair agreement with those reported in the literature [24]. There are no reliable data on the absolute value of the London penetration depth for underdoped samples [25].

Figure 2 shows the ratio  $\Delta W/W_s$  for the samples studied in this work. In the UD sample, we find that at energies as large as  $1 \text{ eV}$  ( $8000 \text{ cm}^{-1}$ ),  $\Delta W/W_s \sim 0.65 \pm 0.18$  (details about the evaluation of the error bars are given further). It approaches 1 at  $\sim 16000 \text{ cm}^{-1}$ . A large part ( $\sim 30\%$ ) of the superfluid weight in the underdoped regime thus builds up at the expense of spectral weight coming from high-energy regions of the optical spectrum ( $\hbar\omega \geq 1 \text{ eV}$ ). Because of our error bars, we cannot make a similar statement for the OPD and OD samples, where the sum rule may be exhausted at roughly  $500\text{--}1000 \text{ cm}^{-1}$ . Our results for the OD and OPD samples thus do not contradict earlier similar work in  $\text{YBa}_2\text{Cu}_3\text{O}_{7-\delta}$  (Y-123) and  $\text{Tl}_2\text{Ba}_2\text{CuO}_{6+\delta}$  (Tl-2212) [5]. Underdoped Y-123 showed a conventional behavior, possibly because only one spectrum is usually recorded in the visible range which is precisely the energy range which matters in this case [16].

The remarkable behavior of the UD sample must be critically examined in light of the uncertainties that enter in the determination of the ratio  $\Delta W/W_s$ . The determination of  $\Delta W$  assumes that  $W(T_A)$  is a fair estimate of the spectral weight obtained at  $T_B < T_c$ , defined as  $W_n(T_B)$ , if the system could be driven normal at that temperature. While this assumption is correct in BCS superconductors, it may no longer be valid for high- $T_c$  superconductors [8], hence our taking the normal-state spectral weight  $W(T_A \geq T_c)$  instead of  $W_n(T_B)$  (unknown) may bias the sum rule. The error incurred by doing so can be estimated as follows. Figure 3 displays the temperature dependence, from  $300 \text{ K}$  down to  $10 \text{ K}$ , of the relative spectral weight  $W(\omega_c, T)/W(\omega_c, 300 \text{ K})$ , for three selected integration ranges, according to eq. (1). At  $\omega_c = 1000 \text{ cm}^{-1}$ , the normalized spectral weight exhibits a significant increase as the temperature

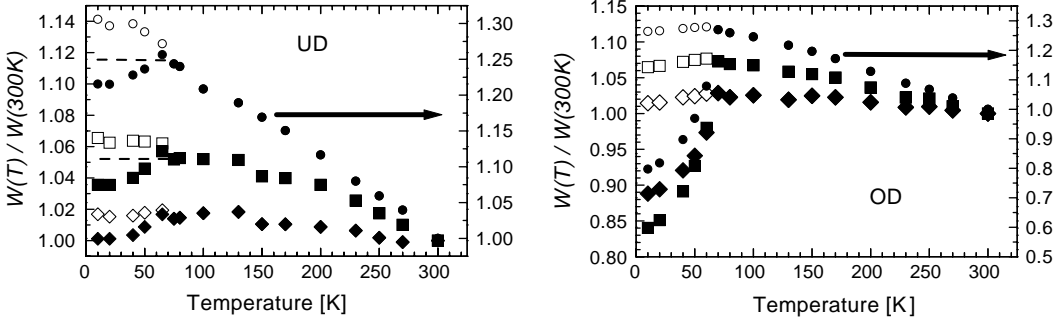


Fig. 3 – Effective spectral weight  $W(T, \omega_c)/W(300\text{ K}, \omega_c)$  vs. temperature for the underdoped (left panel) and overdoped (right panel) samples, at different cutoff frequencies  $\omega_c$  (full symbols).  $\omega_c = 1000\text{ cm}^{-1}$  (circles);  $5000\text{ cm}^{-1}$  (squares); and  $20000\text{ cm}^{-1}$  (diamonds). Open symbols are obtained by adding the superfluid weight  $W_s(T)$  to the spectral weight  $W(T < T_c)$ . The size of the symbols has been adjusted so as to represent the estimated error bar. The dashed lines in the left panel show the approximate location of the open symbols if all the spectral weight had been removed from energy states lying below the associated cut-off frequency (see text).

is lowered, and could therefore keep changing in the superconducting state. One could infer an increase of  $\sim 10\%$  of this relative spectral weight for both samples assuming a linear extrapolation of the data. Hence  $W(T_A)$  is most likely to give too small an estimate for  $W_n(T_B)$  at  $T < T_c$ , in this energy range. To get a better insight of this possible underestimate, the superfluid weight  $W_s(T)$  was added to the spectral weight  $W(T_B)$  (open symbols in fig. 3), at a frequency  $\omega = \omega_c$  and a temperature  $T < T_c$ . Within the experimental uncertainty [26] (represented by the size of the symbols), the normalized spectral weight stays constant from above  $T_c$  at all frequencies for the overdoped sample, and, for the underdoped sample, only at  $20000\text{ cm}^{-1}$  and below  $130\text{ K}$ . This means that the redistribution of spectral weight between the normal and the superconducting state occurs within this range for both samples. In order to estimate the error bars, we have established this plot for a number of cut-off frequencies starting from  $100\text{ cm}^{-1}$ . We extrapolated the data from the temperatures about (but larger than)  $T_c$  in fig. 3, thus inferring an upper bound for  $W_n(T_B)$ . This error becomes negligible at  $5000\text{ cm}^{-1}$ . Above  $5000\text{ cm}^{-1}$ , the uncertainties are those due i) to the error in the relative change of the measured reflectivity with temperature (the error in the absolute value being irrelevant), ii) to the fitting accuracy and iii) to the determination of  $W_s$ . The latter two uncertainties are not independent and must be calculated self-consistently. They yield an upper bound of  $15\%$ - $20\%$  in the uncertainty on the evaluation of  $\Delta W/W_s$ , for all frequencies. All uncertainties are then represented by the error bars in fig. 2. Therefore, the top of the error bars delineates the upper limit for the FGT sum rule at each frequency.

For the UD sample, it is then clear that the low-frequency negative value could be assigned to an incorrect estimate of  $W_n$ . However, the violation of the sum rule for this sample, with  $\Delta W/W_s = 0.65 \pm 0.18$  at  $8000\text{ cm}^{-1}$  is also clearly established. Within the error bars, the sum rule is exhausted in this sample above  $16000\text{ cm}^{-1}$ . The fact that the superfluid involves high-energy states is compatible with the plot below  $T_c$  of the sum of the spectral weight at finite frequency and the superfluid weight (open symbols in fig. 3). Unlike the overdoped sample, where at  $1000\text{ cm}^{-1}$  the spectral weight of the condensate already balances the spectral weight lost up to this frequency, in the UD sample the superfluid spectral weight exceeds the loss at  $1000\text{ cm}^{-1}$  (by roughly a factor of 2). This corresponds to  $\Delta W/W_s$  being of order

50% at this energy, consistent with our data including the error bars (fig. 2). At 5000 cm<sup>-1</sup>,  $\Delta W/W_s \sim 0.6 \pm 0.2$ , and the open symbols are consistently above the normal-state spectral weight (as shown by the dashed lines), implying that there is still some spectral weight coming from higher energy (up to 16000 cm<sup>-1</sup>, as shown in fig. 2).

One interpretation of the sum rule violation can be made in the context of the tight-binding Hubbard model. The relation between the low-frequency spectral weight and the kinetic energy  $E_{\text{kin}}$  per copper site is [16]

$$\frac{\Delta W}{W_s} - \frac{4\pi c}{137\hbar} \frac{a^2}{V} \frac{1}{\Omega_L^2} (E_{\text{kin},s} - E_{\text{kin},n}) = 1, \quad (2)$$

where  $a$  is the (average) lattice spacing in the plane and  $V$  is the volume per site (SI units). This relation means that a breakdown of the FGT sum rule up to an energy  $\hbar\omega_c$  of the order of the plasma frequency ( $\sim 1$  eV for Bi-2212) is related to a change in the carrier kinetic energy  $\Delta E_k = E_{\text{kin},s} - E_{\text{kin},n}$ , when entering the superconducting state. According to our results in the UD sample (fig. 2),  $\Delta W/W_s = 0.65 \pm 0.18$  at 1 eV, which yields  $\Delta E_k = 1.1 \pm 0.3$  meV per copper site. This would be a huge kinetic-energy gain,  $\sim 15$  times larger than the condensation energy  $U_0$ . For optimally doped Bi-2212,  $U_0 \simeq 1$  J/g-at  $\approx 0.08$  meV per copper site [27]. A change of the in-plane kinetic energy could actually drive the superconducting transition, as has been proposed in various scenarios: holes moving in an antiferromagnetic background [28], interlayer tunneling theory [10], or hole undressing [11, 12]. The latter scenario suggests that the violation of the FGT sum rule must be more conspicuous for a dilute concentration of carriers and that, upon doping, a conventional energy scale exhausting the FGT sum rule should be retrieved. Also, the kinetic-energy lowering  $\Delta E_k$  may be much larger than the condensation energy, and was estimated for Tl-2212 to be  $\sim 1$ –3 meV per planar oxygen [7], which results into 0.5–1.5 meV per copper site. It was also suggested that it should be easier to observe the sum rule violation in UD samples in the dirty limit [7], which could apply in our case. A recent scenario also explains our data [13].

STM experiments in optimally doped Bi-2212 samples showed small-scale spatial inhomogeneities, over  $\simeq 14$  Å, which are reduced significantly when doping increases, and whose origin could be local variations of oxygen concentration [29]. Since the wavelength in the full spectral range is larger than 14 Å, the reflectivity performs a large-scale average of such an inhomogeneous medium. The implications in the conductivity are still to be investigated in detail, but it is presently unclear how this could affect the sum rule.

In conclusion, we have found for the in-plane conductivity of the underdoped Bi-2212 a clear violation of the sum rule at 1 eV, corresponding to a kinetic-energy lowering (within the framework of the tight-binding Hubbard model) of  $\sim 1$  meV per copper site. The very large energy scale required in order to exhaust the sum rule in the UD sample cannot be related to a conventional bosonic scale, hence strongly suggests an electronic pairing mechanism.

\* \* \*

We are very grateful to M. NORMAN and C. PÉPIN for illuminating discussions. We acknowledge fruitful comments from J. HIRSCH and E. YA. SHERMAN. We thank P. DUMAS (LURE, Orsay) for his help with the IR microscopy measurements, and A. DUBON and J. Y. LAVAL (ESPCI) for the electron microscopy of the UD sample. AFSS thanks Colciencias and Ministère Français des Affaires Etrangères (through the Eiffel Fellowships Program) for financial support. RPSML acknowledges the financial support of CNRS-ESPCI.

## REFERENCES

- [1] FERRELL R. A. and GLOVER R. E., *Phys. Rev.*, **109** (1958) 1398; TINKHAM M. and FERRELL R. A., *Phys. Rev. Lett.*, **2** (1959) 331.
- [2] See, e.g., RENNER CH. *et al.*, *Phys. Rev. Lett.*, **80** (1998) 149; RANDERIA M. and CAMPUZANO J. C., cond-mat/9709107 (1997).
- [3] BASOV D. N. *et al.*, *Science*, **283** (1999) 49.
- [4] KATZ A. S. *et al.*, *Phys. Rev. B*, **61** (2000) 5930.
- [5] BASOV D. N. *et al.*, *Phys. Rev. B*, **63** (2001) 134514-1.
- [6] TSVETKOV A. A. *et al.*, *Nature*, **395** (1998) 360.
- [7] HIRSCH J. E. and MARSIGLIO F., *Physica C*, **331** (2000) 150; HIRSCH J. E., *Phys. Rev. B*, **62** (2000) 14487.
- [8] CHAKRAVARTY S., *Eur. Phys. J. B*, **5** (1998) 337.
- [9] CHAKRAVARTY S., KEE H.-Y. and ABRAHAMS E., *Phys. Rev. Lett.*, **82** (1999) 2366.
- [10] ANDERSON P. W., *Science*, **258** (1995) 1154.
- [11] HIRSCH J. E., *Physica C*, **199** (1992) 305; **201** (1992) 347.
- [12] HIRSCH J. and MARSIGLIO F., *Phys. Rev. B*, **62** (2000) 15131.
- [13] NORMAN M. R. and PÉPIN C., *Phys. Rev. B*, **66** (2002) 100506.
- [14] FUGOL I. *et al.*, *Solid State Commun.*, **86** (1993) 385.
- [15] HOLCOMB M. J. *et al.*, *Phys. Rev. Lett.*, **73** (1994) 2360.
- [16] VAN DER MAREL D. *et al.*, *Optical signatures of electron correlations in the cuprates, Lecture Notes*, invited talk at the Trieste miniworkshop *Strong Correlation in the high  $T_c$  era, ICTP, Trieste (Italy), 17-28 July 2000*.
- [17] MOLEGRAAF H. J. A. *et al.*, *Science*, **295** (2002) 2239.
- [18] KONSTANTINOVIC Z., LI Z. Z. and RAFFY H., *Physica B*, **259-261** (1999) 569.
- [19] The uncertainty in the thickness given by RBS on films grown on SrTiO<sub>3</sub> is 300 Å.
- [20] MAKSIMOV E. G. *et al.*, *Solid State Commun.*, **112** (1999) 449.
- [21] The best description of our data was obtained by assuming no backward reflection from the rear of the substrate (*i.e.*, assuming an infinitely thick substrate).
- [22] QUIJADA M. A. *et al.*, *Phys. Rev. B*, **60** (1999) 14917.
- [23] SANTANDER-SYRO A. F. *et al.*, *Phys. Rev. Lett.*, **88** (2002) 097005.
- [24] VILLARD G. *et al.*, *Phys. Rev. B*, **58** (1998) 15231.
- [25] DI CASTRO D. *et al.*, *Physica C*, **332** (2000) 405.
- [26] The total spectral weight calculated up to 20000 cm<sup>-1</sup>, including the condensate, is conserved as a function of temperature below 130 K for both samples (fig. 3). The uncertainty is the standard deviation of the 20000 cm<sup>-1</sup> data from 130 K down to 10 K (full symbols above  $T_c$ , open symbols below  $T_c$ ), with respect to the mean value ( $1.045 \pm 0.002$  and  $1.022 \pm 0.005$  for the UD and OD samples, respectively).
- [27] LORAM J. W. *et al.*, *Physica C*, **341-348** (2000) 831.
- [28] BONCA J., PRELOVSEK P. and SEGA I., *Phys. Rev. B*, **39** (1989) 7074; DAGOTTO E., RIERA J. and YOUNG A. P., *Phys. Rev. B*, **42** (1990) 2347; BARNES T. *et al.*, *Phys. Rev. B*, **45** (1992) 256.
- [29] PAN S. H. *et al.*, *Nature*, **413** (2001) 282.